Determining the thermal resistance of a highly insulated wall containing vacuum insulation panels through experimental, calculation and numerical simulation methods

Moore, Travis V.; Cruickshank, Cynthia A.; Beausoleil-Morrison, Ian; Lacasse, Michael

Publisher's version / Version de l'éditeur:
https://doi.org/10.1177/1744259120980032
Journal of Building Physics, pp. 1-21, 2020-12-27

Determining the thermal resistance of a highly insulated wall containing vacuum insulation panels through experimental, calculation and numerical simulation methods

Travis V. Moore[a,b,*], Cynthia A. Cruickshank[b], Ian Beausoleil-Morrison[b], Michael Lacasse[a]

[a] *National Research Council Canada, 1200 Montreal Road, Ottawa, Ontario, Canada, K1A0R6*

[b] *Carleton University, 1125 Colonel By Drive, Ottawa, Ontario, Canada, K1S 5B6*

* *Corresponding author: Travis.Moore@nrc-cnrc.gc.ca, +1 613-949-0194*

1. Abstract

The purpose of this paper is to investigate the potential for calculation methods to determine the thermal resistance of a wall system containing vacuum insulation panels (VIPs) that has been experimentally characterized using a guarded hot box (GHB) apparatus. The VIPs used in the wall assembly have not been characterized separately to the wall assembly, and therefore exact knowledge of the thermal performance of the VIP including edge effect is not known. The calculations and simulations are completed using methods found in literature as well as manufacturer published values for the VIPs to determine the potential for calculation and simulation methods to predict the thermal resistance of the wall assembly without the exact characterization of the VIP edge effect.

The results demonstrate that disregarding the effect of VIP thermal bridges results in overestimating the thermal resistance of the wall assembly in all calculation and simulation methods, ranging from overestimates of 21% to 58%. Accounting for the VIP thermal bridges using the manufacturer advertised effective thermal conductivity of the VIPs resulted in three methods predicting the thermal resistance of the wall assembly within the uncertainty of the GHB results: the isothermal planes method, modified zone method and the 3D simulation. Of these methods only the 3D simulation can be considered a potential valid method for energy code compliance, as the isothermal planes method requires too drastic an assumption to be valid and the modified zone method requires extrapolating the zone factor beyond values which have been validated.

The results of this work demonstrate that 3D simulations do show potential for use in lieu of guarded hot box testing for predicting the thermal resistance of wall assemblies containing both VIPs and steel studs. However, knowledge of the VIP effective thermal conductivity is imperative to achieve reasonable results.

Keywords: Thermal resistance calculation methods, thermal bridges, vacuum insulation panels, guarded hot box, two and three-dimensional heat transfer simulations.

Funding: This work was supported by the Construction Research Centre of the National Research Council of Canada; however this research did not receive any specific grant from funding agencies in the public, commercial, or not-for-profit sectors.

2. Introduction

Determining the effective thermal resistance of a building envelope assembly is an important component in building design. Primarily, the thermal resistance of a building envelope assembly is required to meet a minimum prescriptive value for energy code compliance. Additionally, knowledge of the effective, or apparent, thermal conductivity, specific heat and density of each component in the assembly is necessary to perform whole building energy simulations. The effective thermal resistance is determined as a steady state value, dependent on both the specific temperature difference and surface temperatures at which it is measured as it represents the three modes of heat transfer in a single value (conduction, convection and radiation). The primary method of determining thermal resistance of a wall assembly is through guarded hot box testing, however in many instances calculation methods can be used in lieu of testing.

Historically several calculation methods have been developed and validated through laboratory testing, typically consisting of reducing the thermal resistance of a building envelope system to a one-dimensional (1D) result (Gorgolewski, 2007; Kosny, 1995; ISO 10211-07, 2007; ISO 14683-07, 2007; ISO 6946-07, 2007). For building envelope components in which the system is made of homogenous layers with isotropic properties this typically results in accurate calculations. However, most building envelope assemblies are

non-homogenous containing several materials of differing thermal properties which intersect. In situations where materials of relatively high thermal transmittance dissect highly insulated materials, thermal bridges occur, and heat transfer in two and three dimensions can become dominant. In these situations, 1D calculation methods can result in significant overestimates of thermal performance and additional calculations are necessary.

North American Energy codes, such as the National Energy Code of Canada for Buildings (NECCB) (National Research Council Canada, 2016) and ASHRAE 90.1 (ASHRAE, 2016), reference several methods to determine the thermal resistance of a wall assembly including both experimental and calculation methods (ISO 10211-07, 2007; ISO 6946-07, 2007; ISO 14683-07, 2007). Although accounting for thermal bridges is mentioned in the energy codes, these typically apply to large thermal bridges such as parapets, balconies, or slab edges. Little information is provided to calculate the effect of thermal bridges for individual components in wall assemblies other than framing components, such as steel and wood studs (National Research Council Canada, 2016; ASHRAE, 2016; ASHRAE, 2016). Accounting for individual component thermal bridges in wall assemblies becomes more important as the overall thermal resistance of the assembly increases, which is becoming more common with recent focus on increases to the insulation requirements in energy codes and requirements for up to net-zero construction. Obtaining the high thermal resistances required in these instances, and maintaining achievable wall thickness, leads to use of advanced insulation technologies, such as vacuum insulation panels (VIP). However, the centre of panel thermal conductivity value of a single panel, derived from the partial vacuum in the core material, is not representative of a VIPs actual performance in an assembly due to two main sources of thermal bridges: the barrier film and joints between panels (Simmler, et al., 2005; Schwab, Stark, Wachtel, Ebert, & Fricke, 2005). To maintain the partial vacuum a gas barrier film is required to limit the migration of atmospheric gases and water vapour to the core material and is typically made of metal or metallized components, creating a thermal bridge around the perimeter of the panel itself. As such, the gas barrier film cannot be

perforated which necessitates a combination of panels required for wall construction, to allow for cladding fasteners, duct and pipe penetrations, etc. This causes a second thermal bridge through the joints between panels, as the material in the joints will have a higher thermal transmittance than the centre of the panel (Brunner, Stahl, & Ghazi Wakili, 2012; Lorenzati, Fantucci, Capozzoli, & Perino, 2014; Ghazi Wakili, Bundi, & B.Binder, Effective thermal conductivity of vacuum insulation panels, 2004; Van Den Bossche, Moens, Janssens, & Delvoye, 2010; Simmler, et al., 2005).

Significant work has been completed on determining the effective thermal resistance of VIPs accounting for the thermal bridges, through calculation, simulation and experiments – both in-situ and in the lab.

Nussbaumer et al. (Nussbaumer, Ghazi Wakili, & Tanner, 2006) investigated the performance of VIPs incorporated into a concrete wall system using a guarded hot box and compared the results to numerical simulations with good agreement. The effects of the barrier foil were accounted for by modelling the layers of the foil, and the performance of the VIPs were measured separately using a heat flow meter. They additionally investigated the effects of damaged VIPs and noted that a VIP which had lost its vacuum resulted in a thermal conductivity of 0.020 W/mK. Nussbaumer et al. (Nussbaumer, Bundi, & Muehlebach, 2005) also investigated a wooden door system with undamaged and damaged VIPs, noting that the damaged VIP reduced the overall performance of the door system by 8.5% for a single VIP, and 14% for two damaged VIPs; the damaged VIP had a corresponding thermal conductivity of 0.019 W/m*K. Grynning et al. (Grynning, et al., 2010) performed hot box measurements of several wall structure arrangements of VIPs with various edge and overlap effects and compared the results to numerical simulations. The linear thermal transmittance was calculated in two dimensions in THERM following the methods in ISO 10211. They also measured 20mm and 40mm thick VIPs in both single and double layer configurations in a heat flow meter. The average width of the air gap was simulated as 2mm, however the measured air gap varied from 0mm to 7mm in the experiments. The effect of the air gap was not measured, rather calculated as an equivalent resistance as per ISO 6946. They also noted that a punctured VIP (i.e. loss of vacuum)

resulted in a thermal conductivity of the panel of 20 mW/m*K. Haavi et. al (Haavi, Petter Jelle, & Gustavsen, 2012) measured the thermal resistance of three different wall assemblies containing VIPS, each incorporating different stud profiles and compared the results with numerical simulations. The VIPs were installed between the studs and measured 40mm thick by 600mm wide by 1000mm long with a 0.1mm thick barrier foil and a 0.3mm thick fire retardant barrier. The thermal conductivities of the VIPs were measured as 0.004 W/m*K in a pristine condition, 0.008 W/mK in an aged condition and 0.02 W/MK in a punctured condition. Atsonios et al. (Atsonios, Mandilaras, & Founti, 2019) determined the thermal performance of a novel drywall system insulated with VIPs. The VIPs used in this system were 1.0 m long by 0.60m wide by 0.020m thick. They determined the VIP thermal transmittance and effective thermal conductivity for the panels at two mean temperatures of 10°C and 23°C using a guarded hot plate apparatus. The effective thermal conductivity was measured as 0.00444 and 0.00461 W/m*K at 10°C and 23°C respectively. Fantucci et al. (Fantucci, Lorenzati, Capozzoli, & Perino, 2019) also investigated the temperature dependence of the effective thermal conductivity of 10mm thick VIPs and determined that the thermal conductivity varied from 0.0049 to 0.0075 W/m*K for mean temperatures from -7.5°C to 55.5°C. Berardi et al. (Berardi & Naldi, 2017) investigated the temperature dependence of several insulating materials with a heat flow meter at various mean temperatures, including Fiberglass, Rock-wool, Polyisocyanurate and XPS. For all materials except Polyisocyanurate the temperature dependant thermal conductivity decreases with decreasing mean temperature due to decreases in the contribution of the convection and radiation effects in the overall heat transfer rate.

Sprengard and Holm (Sprengard & Holm, 2014) used numerical simulation to investigate the thermal losses at the edges of panels considering differences in thickness of the panels, type of edge design (single or multilayer foils), inorganic barrier material and thickness of barrier layers, the material used between the joints, and fasteners used to mount the panels, as well as encasement material in various construction types. In general they determined that larger panels are less susceptible to edge losses versus smaller

panels (due to the higher area to perimeter ratio) and that new panels generally exhibited high thermal transmittance values so slightly aged panels should be used for more reasonable values. This work simulated the layers in the foils separately, not as a combined representative value. They determined that the equivalent thermal conductivity for panels measuring 1.0 m in length by 0.5 m in width by 0.02m in depth was 0.051 to 0.074 W/mK depending on the barrier film type. Ghazi Wakili et al. (Ghazi Wakili & Nussbaumer, 2005) used a previously validated numerical model to determine the linear transmittance of two different thicknesses of VIPs in a massive stone wall with floor slab and terrace with continuous transition between inner and outer floors by modelling the multi-layer barrier film as a single representative layer. Additionally, values were produced for VIPs surrounded by 10 mm of insulating material of varying thermal conductivities, ranging from 0.025 to 1 W/m*K. In general the results demonstrate that increasing thickness of the VIP results in a reduced linear thermal transmittance value for the assemblies investigated.

In-situ measurements of the thermal performance of steel stud walls and walls incorporating VIPs has also been investigated. Mandilaras et al. (Mandilaras, Atsonios, Zannis, & Founti, 2014) compared the in-situ performance of a full scale wall clad in ETICs containing both EPS and 0.60m long by 0.40m wide by 0.20 m thick VIPs, with an effective thermal conductivity of 6.3 mW/m*K. Atsonios et al. (Atsonios I. , Mandilaras, Manolitsis, Kontogeorgos, & Founti, 2007) analyzed the in-situ performance of a lightweight steel stud wall incorporating VIPs and used the results to benchmark a whole building simulation model. The resulting model predicted that the VIPs have the potential to reduce the energy demand of the structure by an average of 19% considering the climates of Athens, New York, Oslo and Kuwait. Kontogeorgos et al. (Kontogeorgos, Atsonios, & Mandilaras, 2016) investigated a lightweight steel frame wall incorporating VIPs on the internal surface of a two-storey wall assembly and determined that the VIPs decreased the total thermal transmittance of the structure by 33%. The effective VIP thermal conductivity was determined as 0.007 W/mK.

Several numerical, analytical, and experimental investigations have been used to determine linear thermal transmittances for VIPs in various configurations. Isaia et al. (Isaia, Fantucci, Capozzoli, & Perino, 2016) completed a series of experiments and numerical analysis to develop an empirical model to determine the thermal transmittance of a VIP accounting for the barrier film details, wall assembly insulation configuration and joint material/configuration. In this work the VIP barrier foil was modelled as a single layer, and the bounding layers were modelled as a single representative layer of equivalent thermal conductivity. The air gaps in the joints between VIPs were modelled using an equivalent thermal conductivity following the ISO 6946 simplified method. Tenperik et al. (Tenperik & Cauberg, 2007) developed a method to analytically calculate the corresponding edge thermal transmittance of VIPs accounting for: the heat transmission coefficient at the boundary surface, VIP thickness, laminate thickness, laminate thickness at the panel edge and laminate thermal conductivity. The accuracy was claimed at 5% however, no experimental comparisons were completed. Additionally, the model does not account for air gaps that occur between two abutting VIPs. Van Den Bossche et al. (Van Den Bossche, Moens, Janssens, & Delvoye, 2010) compared the method proposed by Tenpirek to experiment results and determined that the method underestimated the thermal transmittance of the edge values by approximately 8% and 23% for a 20 mm and 30 mm thick panel respectively. The experiment results also determined that methods which do not account for the gap between panels are unreliable. Wakili et al. (Ghazi Wakili, Bundi, & B.Binder, Effective thermal conductivity of vacuum insulation panels, 2004) determined edge thermal transmittance values for 1m by 1m VIPs with two different barrier films containing 90 nm and 300 nm thick metal layers through numerical simulation by combining the multiple thin barrier layers (metal and polymers) into a single layer; the authors caution the use of these results for VIPs of different barrier foil types. Also, the air gap between the VIP panels were not measured, rather ‘adjusted’ in the numerical simulations to tune the numerical results to the experiment results. Lorenzati et al. (Lorenzati, Fantucci, Capozzoli, & Perino, 2014) determined the linear thermal transmittance of 20

mm thick VIPs with three different metallized barriers and four different joint materials (air, XPS, MDF and rubber) between abutting VIPs using a heat flow meter apparatus and normalized the results for various VIP sizes using the perimeter to area ratio.

Overall, the literature review has demonstrated that the effective thermal conductivity of a VIP is dependent on many factors and can easily vary from as low as approximately 4 mW/mK up to 8 W/mK when a partial vacuum is maintained in the core, and up to 20 mW/M*K when the barrier film is punctured. Determining the effective thermal conductivity of a VIP in a wall assembly generically (i.e. without testing the specific assembly) requires detailed knowledge the exact barrier film composition, the temperature difference and global temperatures at which the VIP is tested, the joint material and spacing, the thickness of the panels, type of edge design (single or multiplayer foils), and fasteners used to mount the panels. Having detailed knowledge of each of these factors for a given assembly is unlikely to occur in practice.

Thus, determining the accuracy of typical calculation and numerical simulations using generic material properties (including barrier film effects) in predicting the thermal resistance and condensation risk in comparison to a guarded hot box test provides context for designers, engineers, architects and code officials to judge what level of calculation detail is necessary to provide confidence in the results for energy compliance. Therefore the purpose of this paper is to investigate the potential for industry standard calculation methods, 2D simulations and 3D simulations to be used in predicting the thermal resistance of a wall assembly for which the exact thermal performance of the barrier film is not known. The calculations and simulations were completed with material properties found in either industry standard references, manufacturer advertised values, or literature references (in the case of the temperature dependent thermal conductivities). The results and conclusions will provide guidance to designers, practitioners, and code officials on the potential inaccuracies that can occur from using established

192 calculation methods and simulations with generic material properties, as compared to completing
193 guarded hot box tests on representative wall assemblies containing VIPs and steel studs.

194 3. Calculation Methods

195 The calculation methods used in this paper consist of reducing the heat transfer through a building
196 envelope to a one-dimensional analogous electrical circuit of resistors. The analogous circuit is then
197 reduced to a single combined resistance. The established calculation methods for stud frame
198 construction, from the ASHRAE Handbook of Fundamentals (ASHRAE, 2013), consist of the following:

199 1. Parallel path method
200 2. Isothermal planes method
201 3. Modified zone method

202 Methods 1 and 2 (parallel path, isothermal planes) can be as considered general methods. The parallel
203 path method assumes that heat transfer occurs in the shortest path in the direction of the temperature
204 difference without any contribution from lateral heat flow. The overall thermal resistance is then
205 determined as an area weighted average of the parallel path conductance values. The isothermal planes
206 method assumes that heat transfer is equalized laterally at each material interface before transferring to
207 the next plane, and the total thermal resistance is determine as the sum of thermal resistances of each
208 layer (ASHRAE, 2016). Both of these methods are applicable to a wide variety of wall systems in which the
209 components of the wall assembly have similar thermal transmittance properties. This assumption is not
210 valid for wall assemblies where the majority of heat transfer occurs through thermal bridges (ASHRAE,
211 2011). It has been estimated that using these methods to solve for the thermal resistance of wall
212 assemblies which contain significant heat transfer due to thermal bridges can lead to overestimating the
213 thermal resistance by 20-70% (Morris and Hershfield, 2014).

Method 3, the modified zone calculation method (Kosny, 1995), was developed to account for the effects of steel studs on the thermal resistance of the wall assembly. It accounts for the lateral heat transfer that occurs in the components around the steel stud by determining a "thermally effected zone". This calculation method does account for heat transfer effects due to the thermal bridges caused by the steel studs, however is obviously only applicable to steel stud wall assemblies.

4. Calculation and simulation set-up

The thermal resistance calculations and numerical simulations are completed on a wall assembly that has been previously characterized using a guarded hot box apparatus in accordance with ASTM C1363. The experiment conditions, wall assembly configuration and results are presented in detail in Moore et al. (Moore, Cruickshank, Beausoleil-Morrison, & Lacasse, 2020). This section presents a brief summary of the experiment and wall configuration used to complete the calculations and simulations.

4.1 Wall assembly

The wall assembly consisted of a 2.44 m x 2.44 m x 0.20 m specimen including both steel studs and VIP's. The materials and dimensions used in the wall assembly are listed in Table 1 and a sketch of the layers of the wall assembly is shown in Figure 1, Figure 2 and Figure 3. The wall assembly did not include a cladding.

Table 1: Summary of wall assembly materials and dimensions.

Layer	Description
1	15.875 mm (5/8 in.) Gypsum board
2	6 mil (0.254 mm) polyethylene vapour barrier
3	Mineral fibre insulation (89mm, 3.50 in.)
4	18 gauge (1.09 mm) thick Steel Stud, with fiberglass clips for mounting VIP sandwich panels, spaced at 400mm on centre
5	XPS-VIP-XPS sandwich panel layer (from interior to exterior) – 12.7mm (1/2 in.) XPS, 25mm (1 in.) VIP panel, 50mm (2 in.) XPS.

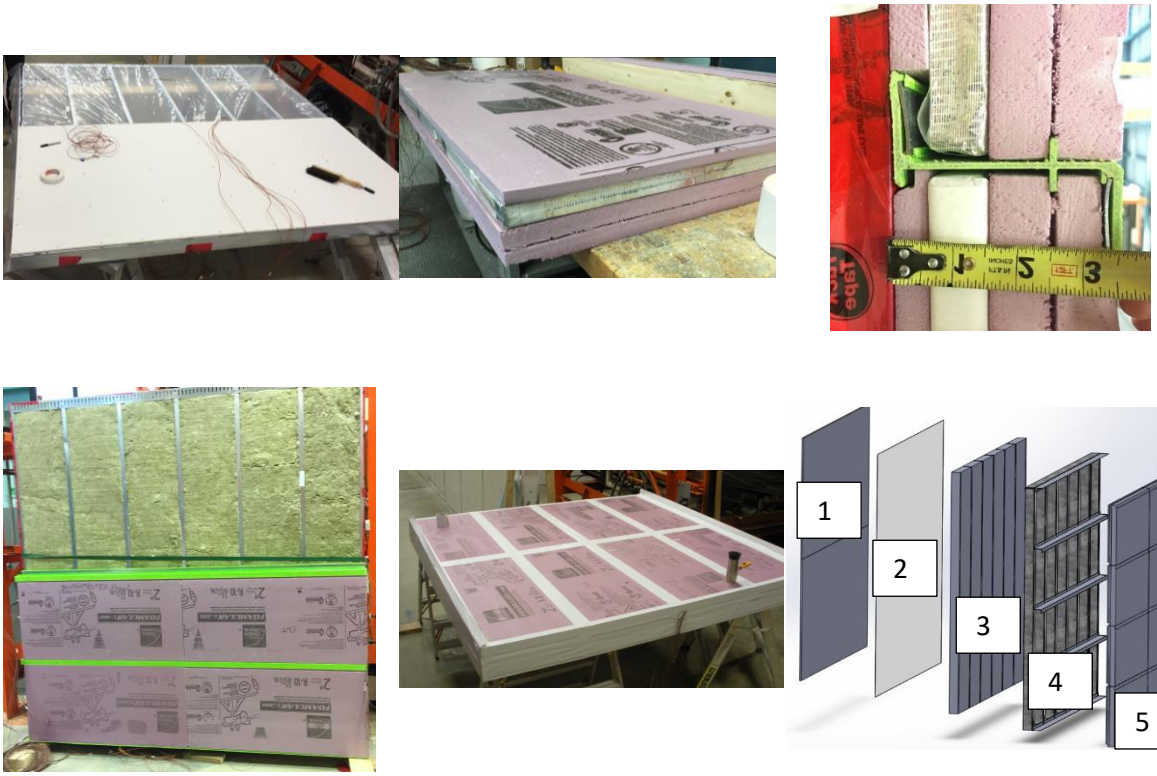

Figure 1: Schematic of wall assembly layers.

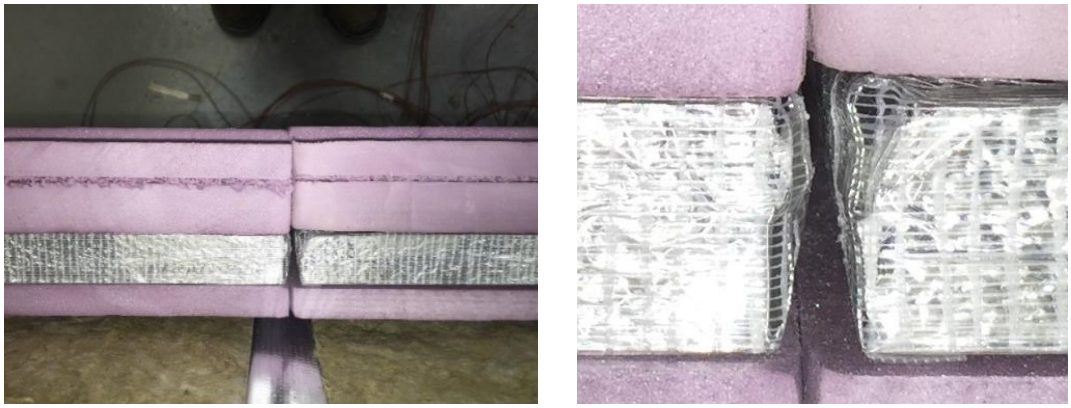

Figure 2: Example of joint width variation between VIPs in wall assembly.

Figure 1 layer 5 represents the XPS (expanded polystyrene)-VIP-XPS sandwich layer, which was made by adhering XPS to the interior and exterior side of 600 mm x 1200 mm x 25 mm VIPs. The XPS layers were added to the VIP to protect the surface from coming in to contact with sharp or abrasive objects, such as

the steel studs, the fiberglass clips holding the panels in place, and the fasteners from the exterior strapping.

4.2 Geometry for industry standard calculation and two-dimensional simulations

The 2D numerical simulations were completed on a plan view of the wall assembly (Figure 3 b, c) and the 3D geometry was drawn based on average measurements in as close an approximation as possible to the actual wall assembly as per the dimensions given previously and in Figure 3. The geometries were drawn in COMSOL (COMSOL AB, 2017). The 2D plan view orientation was selected to account for the effect of thermal bridges due to the steel studs. This orientation assumption ignores thermal bridges that occur due to the fiberglass clips and horizontal air spaces. The effect of this assumption is investigated with the 3D modelling. The air joint between the VIPs in the centre of the wall assembly was measured at several points and is modelled as an average width of 7.44mm, however the air gap width varied from 4.44mm to 11.7mm.

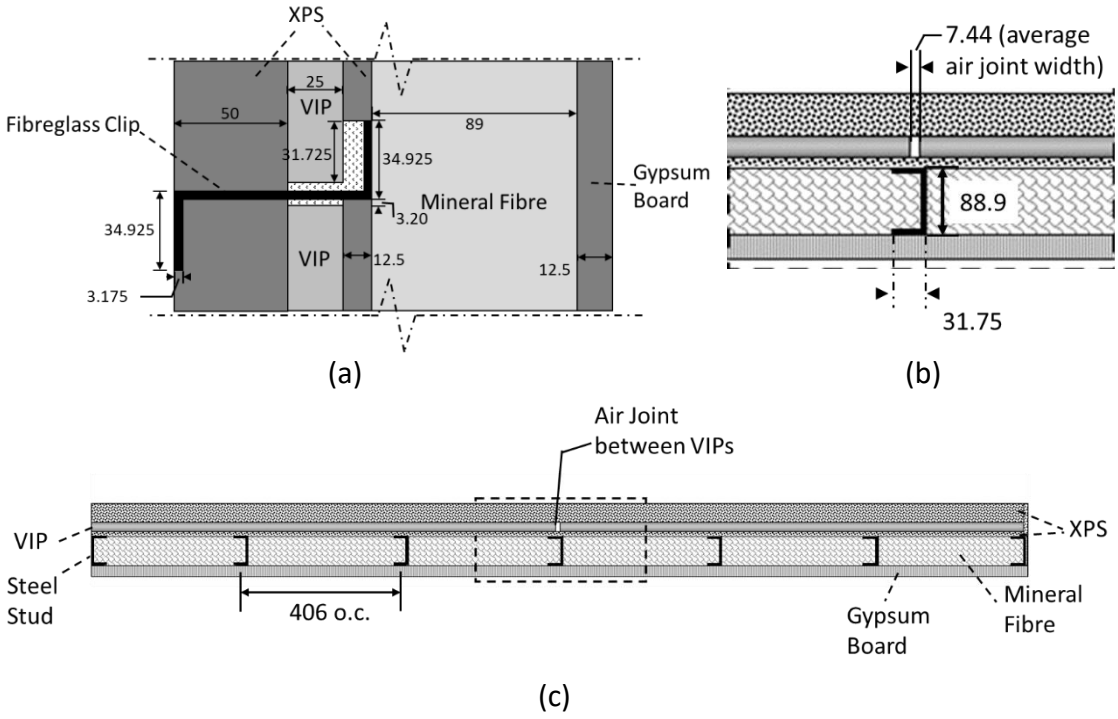

Figure 3: Representative top and side view cross sections depicting the dimensions of the horizontal gaps surrounding the fiberglass clips, all dimensions are in millimetres. (a) Depicts the horizontal air gaps

surrounding the clip at each layer; (b) Depicts a zoom in around the stud and centre VIP gap; (c) shows a top view with each stud location and material labelled

Using the geometry depicted in Figure 3c the assembly was divided up into separate heat transfer paths and isothermal planes for the parallel path method and isothermal planes method respectively, as shown in Figure 4. The modified zone geometry was in the same manner as the isothermal planes method, however the stud cavity was calculated based on the procedure outlined in the ASHRAE Handbook of Fundamentals.

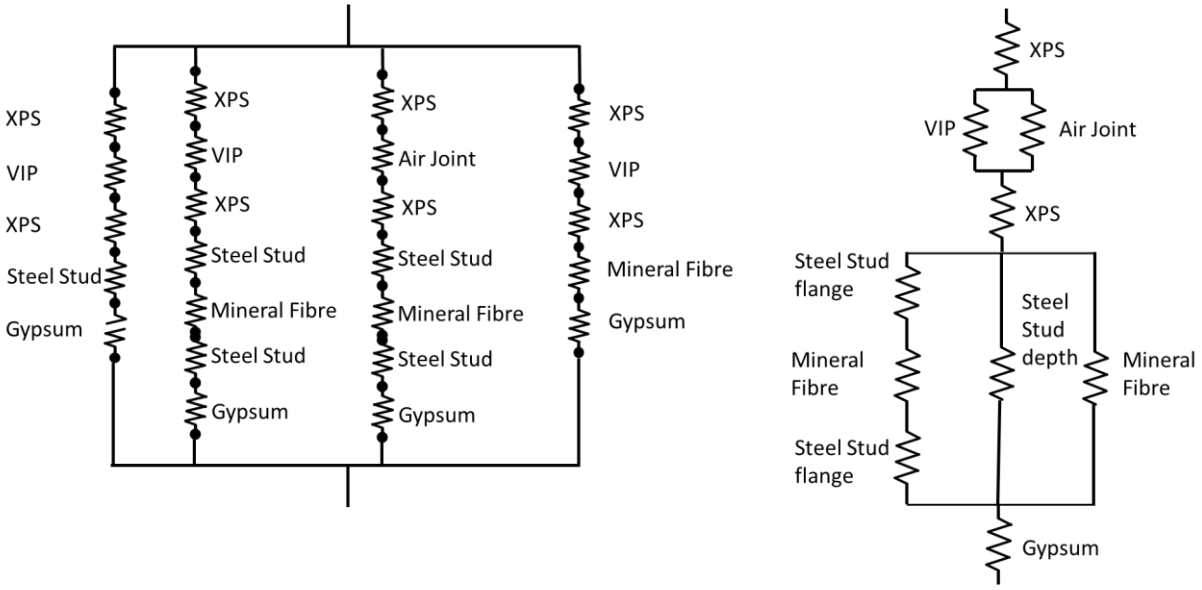

Figure 4: Geometry from Figure 3c divided into respective heat transfer paths for the parallel path method (a), and isothermal planes for the isothermal planes method (b).

4.3 Material properties

The thermal conductivities for all materials are presented in Table 2 and were derived from a combination of industry material properties (ASHRAE, 2013), manufacturer literature and the literature review. The temperature dependent thermal conductivities were used for XPS and mineral fibre, taken from Berardi & Naldi (Berardi & Naldi, 2017). The VIP thermal conductivities were only available from the manufacturer. These consisted of the centre of panel value, which includes no contributions due to the

heat transfer through the barrier foil at the edges of the panel, and the design value which includes adjustments due to heat transfer through the barrier foil at the edges and service life aging. These values are reported to be measured at a mean temperature of 10°C; temperature dependency is not provided. As reported by Fantucci et al. (Fantucci, Lorenzati, Capozzoli, & Perino, 2019) the effective thermal conductivity of VIPs decreases as temperature decreases, so the values used could be considered conservative compared to if the temperature dependent thermal conductivity values were used, as the VIPs are installed in the wall assembly close to the exterior. Temperature dependent thermal conductivities were not available for the gypsum or steel stud; the thermal conductivities for these two materials were obtained from the ASHRAE Handbook of Fundamentals.

Table 2: Effective thermal conductivities

Material	Reference	Effective thermal conductivity [W/mK]
XPS	Berardi & Naldi (Berardi & Naldi, 2017)	k = 0.00014*T[°C] + 0.02602
Steel stud (18 gauge)	ASHRAE Handbook of Fundamentals	48.0
Mineral fibre	Berardi & Naldi (Berardi & Naldi, 2017)	k = 0.00014*T[°C] + 0.03150
Gypsum	ASHRAE Handbook of Fundamentals	0.16
VIP	Manufacturer centre of panel value, "CoP"	0.0042
	Manufacturer design effective VIP thermal conductivity, "VIP_eff"	0.0061

4.3.1 Air joint material properties

The air joint material properties were determined using the method outlined in ISO 6946 Annex B.4 as per Isaia et al. (Isaia, Fantucci, Capozzoli, & Perino, 2016) and (Grynning, et al., 2010). The dimensions used to calculate the effective thermal resistance of the air space were taken based on the largest air joint corresponding to the vertical joint between the VIPs at each layer. The dimensions consisted of an average

air joint width of 7.44 mm, a depth of 25 mm, and a height of 600mm. The average temperature of and temperature difference across the airspace were determined by extracting data from the 3D simulation with the air space modelled as purely conductive heat transfer. The thermal conductivity of the air in the 3D simulation used the temperature dependent thermal conductivity native to the COMSOL material property database. This resulted in an average air temperature of -6.6°C and a temperature difference across the air space of 18.38°C. Using these values and the procedure in ISO 6946 Annex B.4 resulted in an equivalent thermal conductivity of the airspace of 0.096 W/mK. This was implemented into the final 3D model by multiplying the COMSOL temperature dependent thermal conductivity curve by a scaling factor of 4.05. The scaling factor was determined by dividing the effective thermal conductivity determined using the ISO 6946 Annex B.4 procedure by the corresponding air thermal conductivity value in COMSOL at a temperature of -6.6°C. One aspect not accounted for in this analysis is the potential for air to circulate around the corner of the VIP, given that the air joints on the top and bottom of the VIP is connected to the vertical air joint. It is assumed that the potential for the air to wrap around the corner of the VIP does not have a significant effect on the overall thermal resistance of the wall assembly.

4.3.2 Barrier film description

The manufacturer describes the barrier film in the VIPs used in the experiments as a tri-layer aluminized film with a total thickness of 97 microns (0.097mm) consisting of three layers of aluminized olyester and a single layer of linear low density polyethylene for heat sealing. The core material is made up of opacified silica consisting of pyrogenic silica and a silicon carbide based opacifier with reinforcing fibers made of glass, polyester or cellulose. There are no getters in the core material. No information is provided on the orientation or individual thickness of the layers in the barrier film. The design thermal conductivity is reported as 0.0061 W/m*K and is stated to account for both the thermal bridges at the edges of the panel due to the barrier foil and an adjustment for service life. Comparing this value to the range of values in

the literature review (0.003 to 0.008 W/mK) shows that this value seems in the appropriate range for thermal bridging effects.

4.4 Numerical simulation governing equations

The numerical simulations were completed assuming all heat transfer through the solid components was due to conduction. The simulations solved the general governing equation for heat conduction (COMSOL AB, 2017), given for one dimension in Equation 1.

$$q" = -\lambda * \frac{dT}{dx} \qquad \textbf{Equation 1}$$

$q"$ – heat flux [W/m^2]
λ – thermal conductivity [W/mK]
dT – temperature difference between nodes [K]
dx – length between nodes [m]

4.4.1 Boundary conditions

The boundary conditions (BCs) in the numerical models were implemented as per the BC's from in the GHB testing described in Moore et al. (Moore, Cruickshank, Beausoleil-Morrison, & Lacasse, 2020).

During the GHB test the surfaces of the wall assembly was exposed to three different boundary conditions. The interior surface is exposed to the metering box air, the exterior surface is exposed to weather side air, and the lateral surfaces are exposed to the insulated mask.

The interior and exterior surface boundary conditions were assumed to be the average surface heat flux coefficients (determined using characterization specimens as per ASTM C1363) and the ambient air temperatures for each side of the GHB. The boundary conditions for the interior and exterior surfaces are presented in Table 3. The modelling imposes the surface heat flux coefficient and the ambient temperature and solves for the corresponding surface temperature and heat flux using conservation of energy at the surface, as shown in Equation 2.

$$\lambda\left(\frac{T_{y-1}-T_y}{dy}\right)=h_s(T_y-T_\infty) \qquad \textbf{Equation 2}$$

λ – is the apparent thermal conductivity of the material [W/mK]
T_{y-1} – is the temperature at the previous element to the surface [°C]
T_y – is the temperature at the surface element [°C]
dy – is the distance between the elements [m]
h_s – is the average surface heat flux coefficient from the GHB characterization tests [W/m^{2}k]
T_∞ - is the ambient temperature of the air during the VIP wall GHB tests [°C]

Table 3: Interior and exterior boundary conditions.

Interior air temperature [°C]	20.9
Interior heat flux coefficient [W/m^{2}K]	6.6
Exterior air temperature [°C]	-34.9
Exterior heat flux coefficient [W/m^{2}K]	8.4

The lateral surfaces of the specimen in the GHB are in contact with an insulated mask, assumed to be a perfect thermal insulation condition, with zero heat flux normal to the lateral edges. This is represented in the model as shown Equation 3.

$$\lambda\left(\frac{T_{x-1}-T_x}{dx}\right)=0 \qquad \textbf{Equation 3}$$

λ – is the apparent thermal conductivity of the material [W/mK]
T_{x-1} – is the temperature at the previous element to the surface [°C]
T_x – is the temperature at the surface element [°C]
dx – is the distance between the nodes [m]

5. Calculation and simulation results and uncertainty

This section presents the comparison between the calculated and simulated thermal resistance of the wall assembly to the GHB experiment result. Additionally, this section presents the estimated uncertainty of the experiment, calculation and simulation results.

5.1 Uncertainty

The uncertainty of the GHB test results was determined for the temperature measurements and the thermal resistance calculation. The combined thermocouple uncertainty was determined as ±0.45°C, and the combined uncertainty in the thermal resistance of the GHB test was ±11.7%. Further detail on the thermal resistance uncertainty can be found in Moore et. al (Moore, Cruickshank, Beausoleil-Morrison, & Lacasse, 2020).

The overall uncertainty for the industry standard calculation methods was determined as +/-5.5%. This estimate is made based on the estimated combined uncertainty of ±2% for the material properties which were measured by a heat flow meter (Lackey, Normandin, Marchand, & Kumaraman, 1994; Berardi & Naldi, 2017), plus an assumed +/-3% for the potential VIP panel thermal conductivity uncertainty and an uncertainty caused by the variance in air joint width of +/-0.5% (this was determined in the 3D simulations). There could be considerable higher uncertainty due to the VIP thermal conductivity given other measurements in literature and given that this component provides a significant portion of the thermal resistance to the wall assembly.

Similarly the uncertainty in the 2D simulation results is estimated at +/-5.5% considering uncertainty due to the material properties, discretization of the geometry, convergence and rounding of the numerical solution. The uncertainty due to the discretization, convergence and rounding error of the numerical solution is estimated from the difference between the heat flux in to and heat flux out of the geometry. It is assumed that discretization error is negligible in this case, as the difference in heat fluxes are less than 0.1%. The convergence of the simulations is 0.001% and is also assumed to not significantly increase the uncertainty of the simulation results.

The 3D simulation uncertainty is estimated as +/-6.5% and considers uncertainty due to the material properties, discretization, convergence and rounding of the numerical solution. The increased uncertainty

in the 3D results compared with the 2D results is from the mesh convergence of the 3D numerical simulations resulting in a slight difference between the heat flux in to and out of the assembly due to the mesh being limited in the number of elements, of approximately ±1.0%.

5.2 Results and discussion

The thermal resistance calculation and simulation methods are compared to the guarded hot box test results for two cases. The first case is using the centre of panel thermal conductivity from the manufacturer, so these values do not include any contributions due to the thermal bridges at the edges of the panel. The second case is using the manufacture advertised design value, which is stated to include contributions due to both the thermal bridges due to the barrier film edges and a service life aging factor. Additionally, the surface temperature around the steel stud is compared between the three- dimensional simulation results and the GHB measurements. These values help indicate the potential for determining condensation risk due to the studs on the interior surface using calculation methods. All experiment results are described in further detail in Moore et al. (Moore, Cruickshank, Beausoleil-Morrison, & Lacasse, 2020).

5.2.1 Thermal Resistance Comparison

The results of each thermal resistance calculation method (parallel path, isothermal planes and modified zone method) and the two- and three-dimensional numerical simulations are provided in Figure 5. As discussed the results for each method are presented for two cases of VIP thermal conductivity: with (VIP 0.0061) and without (VIP 0.0042) accounting for barrier foil thermal bridges. As could be expected, all calculations and simulations that did not account for thermal bridges due to the barrier film resulted in significant overestimates of the thermal resistance. For instance, in a worst case scenario, completing a 1D calculation neglecting all thermal bridge effects (steel studs, fibreglass clips, air joints and VIP barrier

397 film) results in a thermal resistance of 11.3 m^2K/W, indicating that the effects due to thermal bridges in
398 this wall assembly reduce the potential thermal resistance by 40% as compared to the GHB test result.

399 Comparing the calculation results with the results from the guarded hot box show that no results are
400 within the upper limit of the uncertainty of the GHB results. The closest value to the experiment results is
401 from the isothermal planes, with an overestimate of 21%, followed by the 3D results which overestimates
402 by 24%. The parallel path method results in the highest overestimate, not surprising considering it does
403 not account for any lateral heat transfer effects, with an overestimate of 58%. The modified zone method
404 results in an overestimate of 40% and the 2D simulation results in an overestimate of 53%.

405 Considering the results that account for the thermal bridges at the edges of the VIP shows a much better
406 comparison to the experiment results. In all, three of the methods give results within the uncertainty of
407 the experiment result: the isothermal planes method, the modified zone method and the 3D simulations.
408 The parallel path method overestimates the experiment result by approximately 31% and the 2D
409 simulation overestimates the experiment result by approximately 28%.

410 Considering these results, it would seem that the most accurate method to determine the thermal
411 resistance would be the isothermal planes method, as this results in the least overestimate when thermal
412 bridges are not considered, and is within the uncertainty of the experiment results when thermal bridges
413 are considered. This is an unexpected result, as although this method does account for the potential of
414 lateral heat transfer, the 2D geometry that the calculation is completed over does not account for the
415 thermal bridging due to the horizontal fiberglass clips, bottom track stud or top track stud so one would
416 have expected it to still overestimate the thermal resistance of the wall assembly. However, analyzing the
417 thermal resistance breakdown given in Figure 4 demonstrates that these results are not valid, as the
418 reason for the low thermal resistance estimate is due to a significant underestimate of the contribution
419 to the thermal resistance from the mineral fibre insulation. This is due to the base assumption of the

method that all heat transfer occurs laterally within a given plane in the wall assembly, which in this case is too extreme. The other calculation result that shows promise from the results considering thermal bridges is the modified zone method. However, determining the thermal resistance of the wall assembly using the modified zone method required extrapolating the zone factor beyond that which was validated in its development. Therefore, further validation on other steel stud wall assemblies with VIPs is required before this method can be recommended as a valid calculation method for steel stud wall assemblies with VIP insulation on the exterior.

Comparing the results of the simulations demonstrates that the 2D simulation overestimates the thermal resistance in both cases. The most likely reason for this is due to the 2D geometry neglecting the heat transfer due to thermal bridges due to the horizontal components (fiberglass clips, top track stud, and bottom track stud), as well as the horizontal air joints.

The 3D simulations do account for the horizontal thermal bridges mentioned, and correspondingly when the thermal bridges due to the barrier foil are accounted for predicts a thermal resistance within the uncertainty of the experiment result. However, performing the 3D simulations does require significant detail of the wall assembly being tested, including the width of all joints surrounding the VIP panel. Given that the 3D result predicts a thermal resistance that is at the higher end of the uncertainty band of the experiment results, one could conclude that the true effective thermal conductivity of the VIP including thermal bridges is slightly higher than that used in the simulations. This provides evidence, as discussed in the literature review, the fact that accurate calculations and simulations of wall assemblies that incorporate VIPs need measured data of the actual VIP used in the wall assembly to provide the most confidence in the calculated/simulated results. Additionally, comparing the 3D simulation results between the centre of panel (VIP 0.0042) and effective (VIP 0.0061) thermal conductivities indicates that a reduction in the thermal bridge effect due to the barrier films could improve the overall wall performance by approximately 12%. Comparing the calculated effective thermal conductivity of the airspace between

444 the VIPs and to the centre of panel thermal conductivity (0.096 to 0.0042 W/m*K) also indicates that
445 reducing the air gap between the VIPs would result in improved thermal resistance of the wall assembly.
446 These improvements to the wall design could be achieved by more tightly butting the VIPs and by using
447 two staggered (offset joints) layers of thinner VIPs instead of the single layer VIP used in this wall assembly,
448 as was explored by Brunner et al. (Brunner, Stahl, & Ghazi Wakili, 2012).

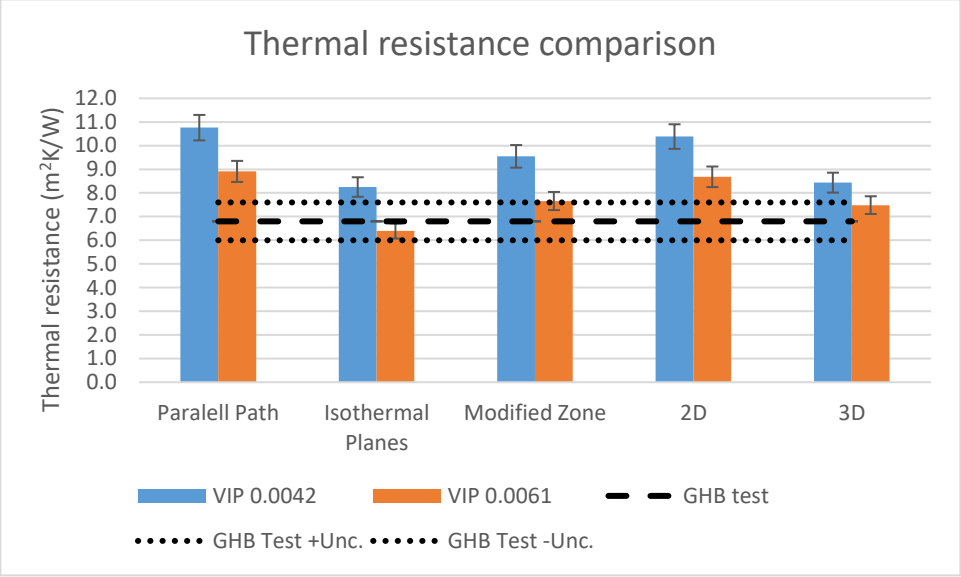

449 **Figure 5: Thermal resistance results comparing industry standard calculations and two and three-dimensional**
450 **simulations to guarded hot box test results.**
451

452 ### 5.2.2 Steel stud effect on interior surface temperature

453 The interior surface temperature in proximity to the steel stud was also compared between the 3D
454 simulation which considered thermal bridges due to the VIP and the experiment. The temperature in
455 proximity to the stud is an important indicator of the potential for condensation to occur due to the steel
456 studs. The comparison is shown in Figure 6, and demonstrates that the 3D simulation can accurately
457 predict the surface temperature in proximity to the steel stud within the uncertainty of the experiment.
458 This indicates that 3D simulations can be used to determine the potential for condensation with good
459 agreement to the experiment.

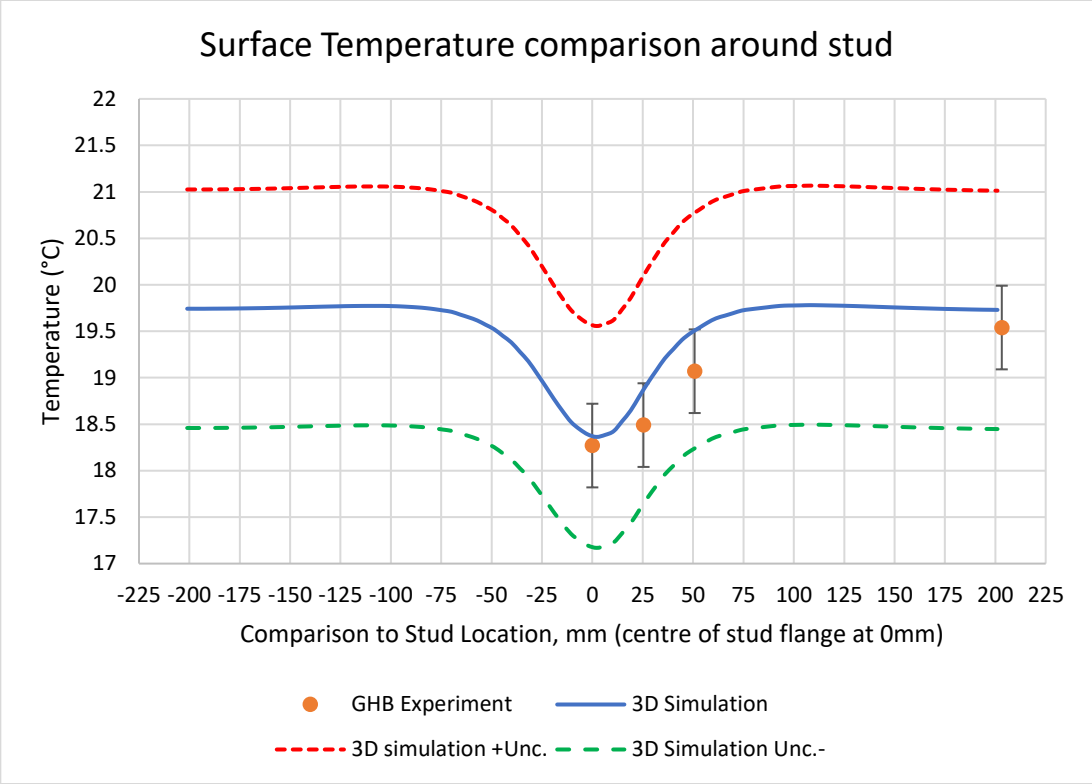

Figure 6: Comparison of the surface temperature in proximity to the steel stud between the 3D simulation and the experiment.

6. Conclusions

This paper presented the results of typical standard calculation methods and two- and three-dimensional simulations in determining the thermal resistance of a wall assembly that incorporates both VIPs and steel studs and was characterized in a guarded hot box. In addition to the thermal bridges due to the barrier film in the VIP and the steel studs the wall assembly also included thermal bridges due to horizontal fiberglass clips used to hold the insulation on the exterior of the wall assembly and air joints surrounding the VIPs.

The calculations and simulations were completed for two VIP thermal conductivity scenarios, both from the manufacturer data. The first scenario used the centre of panel thermal conductivity, meaning it did not account for any thermal bridging around the panels. The second scenario used the manufacturer

advertised design value, which included contributions due to the thermal bridging of the barrier foil at the panel edges. The exact barrier film composition for the VIPs used in the wall assembly were not known, and the VIP was unable to be characterized separately due to limitations in test equipment. This scenario would be representative of a designer, engineer or code official who is seeking to evaluate the potential use of VIPs in a wall system for energy code compliance.

As might be expected, the results for the calculations and simulations for the scenario in which the thermal bridges due to the barrier films in the VIPs were not accounted for resulted in significant overestimations of the wall thermal resistance, ranging from a 21% overestimation to a maximum overestimation of 58%.

For the scenario considering the barrier film thermal bridges three methods predicted the thermal resistance of the wall assembly within the uncertainty of the experiment: specifically, the isothermal planes method, the modified zone method and the 3D simulation. However, the isothermal planes method result was deemed not applicable, as due to the drastic assumption of complete lateral heat transfer at each layer it grossly underestimated the contribution of the mineral fibre insulation to the overall thermal resistance of the wall assembly. Due to the high level of exterior insulation in the wall assembly from the VIPs, the modified zone method required extrapolation of the zone factor – beyond that which had been validated during its development. Therefore more validation with other wall assemblies is needed before this calculation method can be considered valid for use in energy compliance calculations of steel stud wall assemblies with VIP exterior insulation.

The 3D simulations also predicted the thermal resistance of the wall assembly within the uncertainty of the experiment, and from the results in this paper can be considered a viable method of determining thermal resistance of a wall assembly containing steel studs and VIPs in lieu of testing for energy code compliance. However, specific details of the wall assembly are required, especially regarding the VIP effective thermal conductivity and the joints between VIP panels. Additionally, the interior surface

temperature in proximity to the steel stud was compared between the 3D simulations and the experiment. The results of this comparison also indicate that 3D simulations can predict the surface temperature of these type of wall assemblies within the uncertainty of a GHB experiment and can be considered valid for assessing the potential for the steel stud to cause condensation on the interior surface.

7. Acknowledgments/Declarations

This work was completed with the support of the National Research Council of Canada, however this institution did not have influence in study design; in the collection, analysis and interpretation of data; in the writing of the report; nor in the decision to submit the article for publication.

8. References

ASHRAE. (2011). *RP-1365 Thermal Performance of Building Envelope Details for Mid- And High-Rise Buildings.* ASHRAE.

ASHRAE. (2013). *2013 ASHRAE Handbook Fundamentals.* Atlanta, GA, U.S.: ASHRAE.

ASHRAE. (2016). *ANSI/ASHRAE/IES Standard 90.1-2019 -- Energy Standard for Buildings Except Low-Rise Residential Buildings.* Atlanta, GA: ASHRAE.

ASHRAE. (2016). *ASHRAE Handbook of Fundamentals.* Atlanta, GA: ASHRAE.

Atsonios, I., Mandilaras, I., & Founti, M. (2019). Thermal Assessment of a Novel Drywall systm Insulated with VIPs. *Energies , 12*, 18.

Atsonios, I., Mandilaras, I., Manolitsis, A., Kontogeorgos, D., & Founti, M. (2007). Experimental and Numerical investigation of the Energy Efficiency of a Lightweight Steel Framed building incorporating Vacuum Insulation Panels. *6th International Energy in Buildings Conference*.

Berardi, U., & Naldi, M. (2017). The impact of temperature dependant thermal conductivity of insulating materials on the effective building envelope performance. *Energy and Buildings, 144*, 262-275.

Brunner, S., Stahl, T., & Wakili, K. G. (2012). Single and double layered vacuum insualtion panels of the same thickness comparison. *Building Enclosure Science Technology Conference (BEST3).* Atlanta.

COMSOL AB. (2017). *COMSOL Multiphysics(R) v. 5.2.* Stockholm, Sweden: COMSOL AB.

Fantucci, S., Lorenzati, A., Capozzoli, A., & Perino, M. (2019). Analysis of temperature dependance of the thermal conductivity in Vacuum Insulation Panels. *Energy & Buildings, 183*, 64-74.

Ghazi Wakili, K., & Nussbaumer, T. B. (2005). Thermal Performance of VIP assemblies in Building Constructions. *7th Itnernational Vacuum Insulation Symposium*, 131-138.

Gorgolewski, M. (2007). Developing a simplified method of calculating U values in light steel framing. *Building and Environment, 42*, 230-236.

Grynning, S., Petter Jelle, B., Uvslokk, S., Gustavsen, A., Baetens, R., & Meloysund, V. (2010). Hot Box investigations and theoretical assessments of miscellanious vacuum insulation panel configurations in building envelopes. *Journal of Building Physics, 34*(4), 297-324.

Haavi, T., Petter Jelle, B., & Gustavsen, A. (2012). Vacuum insulation panels in wood frame wall constructions with different stud profiles. *Journal of Building Physcis, 36*(2), 121-226.

Isaia, F., Fantucci, S., Capozzoli, A., & Perino, M. (2016). Thermal bridges in vacuum insulation panels at building scale. *Engineering Sustainability, 170*(ES1), 47-60.

ISO 10211-07. (2007). *Thermal bridges in building constructions - Heat flows and surface temepratures - Detailed Calculations.* Geneva, CH: ISO.

ISO 14683-07. (2007). *Thermal bridges in building construction - Linear thermal transmittance - Simplified methods and default values.* Geneva, CH: ISO.

ISO 6946-07. (2007). *Building components and building elements -- Thermal resistance and thermal transmittance -- Calculation method.* Geneva, CH: Internation Organization for Standardization.

Kontogeorgos, D., Atsonios, I., & Mandilaras, I. F. (2016). Numerical investigation of the effect of vacuum insulation panels ont eh thermal bridges of a lightweight drywall envelope. *Journal of Facade Design and Engineering 4*, 3-18.

Kosny, J. (1995, July). Comparison of Thermal Performance of Wood Stud and Metal Frame Wall Systems. *Thermal Insulation and Budiling Environments, 19*.

Lackey, J., Normandin, N., Marchand, R., & Kumaraman, M. (1994). Calibration of a Heat Flow Meter Apparatus. *Journal of Thermal Insulation and Buidling Envelopes*, 128-144.

Lorenzati, A., Fantucci, S., Capozzoli, A., & Perino, M. (2014). The effect of different materials joint in vacuum insulation panels. *6th International Conference on Sustainability in energy and Buidlings*, (pp. 374-381).

Mandilaras, I., Atsonios, I., Zannis, G., & Founti, M. (2014). Thermal performance of a building envelope incorporating ETICS with vacuum insulation panels and EPS. *Energy and Buildings 85*, 654-665.

Moore, T., Cruickshank, C., Beausoleil-Morrison, I., & Lacasse, M. (2020). Thermal evaluation of a highly insulated steel stud wall with vacuum insulation panels using a guarded hot box apparatus. *Journal of Building Physics - Accepted, under revision*, 21.

Morris and Hershfield. (2014). *Building Envelope Thermal Bridging Guide.*

National Research Council Canada. (2016). *National Energy Code for Buildings Canada.* Ottawa, ON: National Research Council Canada.

Nussbaumer, T., Bundi, R. T., & Muehlebach, H. (2005). Thermal analysis of a wooden door system with integrated vacuum insulation panel. *Energy and Buildings 37*, 1107-1113.

Nussbaumer, T., Ghazi Wakili, K., & Tanner, C. (2006). Experimental and numerical investigation of thermal perfromance of a protected vacuum-insulation system applied to a concrete wall. *Applied Energy 83*, 841-845.

Schwab, H., Stark, C., Wachtel, J., Ebert, H.-P., & Fricke, J. (2005). Thermal Bridges in Vacuum-insulated Building Facades. *Journal of Thermal Env. and Bldg. Sci.*, 345-355.

Simmler, H., Brunner, S., Heinemann, U., Schwab, H., Kumaran, K., Mukhopadyaya, P., . . . Stramm, C. T. (2005). *Vacuum Insulation Panels - Study on VIP Components and PAnels for service Life Prediction in Building Applications (Subtask A).* International energy agency. Switzerland: EMPA.

Simmler, H., Brunner, S., Heinemann, U., Schwab, H., Kumaran, M. K., Mukhopadhyaya, P., . . . Kucukpinar-Niarchos, E. (2005). *International Energy Agency Annex 39: High Performance Thermal Insulation Materials, Subtask A: Vacuum insulation panels - study on VIP-components and panels for service life prediction of VIP in building applications.* Paris, France: IEA/ECBCS.

Sprengard, C., & Holm, A. (2014). Numerical examination of thermal bridging effects at the edges of vacuum insulation panels (VIP) in various constructions. *Energy and Buildings 85*, 638-643.

577 Tenperik, M., & Cauberg, H. (2007). Effects Caused by Thin High Barrier Envelopes around Vacuum
578 Insulation Panels. *Journal of Building Physics*.

579 Van Den Bossche, N., Moens, J., Janssens, A., & Delvoye, E. (2010). *Thermal Performance of VIP panels:*
580 *Assessment of the edge effect by experimental and numerical analysis.* Ghent: Ghent University,
581 Department of Architecture and Urban Planning.

582 Wakili, K. G., Bundi, R., & B.Binder. (2004). Effective thermal conductivity of vacuum insulation panels.
583 *Building Research and Information*, 293-299. doi:10.1080/0961321042000188644

584